Adsorption (2024) 30:1467–1478
https://doi.org/10.1007/s10450-024-00517-z

Production of activated carbons from *Quercus cerris* acorn shell under various experiment conditions, and their characterizations

Cengiz Çesko[1] · Ünal Geçgel[2] · Hyrije Koraqi[1] · Osman Üner[3] · Demokrat Nuha[1] · Berat Durmishi[1] · Roland Daci[1] · Diellëza Elshani[1] · Hatice Palüzar[2]

Received: 26 May 2024 / Revised: 24 June 2024 / Accepted: 26 June 2024 / Published online: 15 July 2024

Abstract
Due to the high porosities, large surface areas, insolubilities in solutions, and unique structural and morphological structures, porous materials are utilized in various application areas such as energy conversion and storage, wastewater treatment, adsorption, catalysis and photocatalysis. In this study, activated carbons (QCACs), one type of porous materials, were synthesized from *Quercus cerris* acorn shells by using $ZnCl_2$ chemical activation under various production conditions. The effects of carbonization temperature, carbonization period, and impregnation ratios on the yields, surface areas, pore developments, and N_2 adsorption–desorption isotherms of activated carbons obtained were investigated in detail. The highest surface area (1751.61 m^2/g) was reached when utilized at the impregnation ratio of 2.0 at 500 °C for 90 min. The total pore volume of QCAC increased with increasing impregnation ratio, however the micropore volume of QCAC reduced. It was found from the pore distribution data that QCACs contained mostly narrow mesopores and a little amount of micropores. Also, N_2 adsorption–desorption isotherm data revealed that QCACs produced under different conditions were usually mesopore structures, and the pores were narrow slit-shaped. Moreover, the data provided from SEM, FTIR, Boehm titration, and elemental analysis gave more characterization information about QCACs synthesized.

Keywords Activated carbon · BET surface area, Porosity · Pore size distribution · Boehm titration · *Quercus cerris* L.

1 Introduction

The need for clean water for living bodies and nature is increasing day by day due to the high population growth and unconscious industrial activities. Higher than 1.0×10^5 tons of pigments and dyes are globally produced each year and it has been stated to be major contributor to water pollution compared to other pollutants [1]. In the dyeing processes of textile industry, almost 10–15% of the dye is missing each year, and releases in wastewater [1, 2]. Other toxic pollutants in water resources, such as heavy metals, drugs, pesticides, industrial chemicals, surfactants, etc., also damage the ecological balance, increase environmental pollution dramatically, and hence adversely influencing biological living systems [3, 4]. To prevent water pollution and facilitate access to clean usable water around the world, it is crucial to reduce domestic or untreated industrial effluents polluting our water resources or take protective measures.

Various techniques, such as adsorption, ion exchange, biological treatment, oxidation, membrane filtration, etc., have been studied for wastewater treatments [5–7]. Comparatively, adsorption provides cost-effective, usage ease and simplicity of design; therefore, it is regarded as one of the most influential methods for water treatment processes [8–10]. In the adsorption processes, the selection of adsorbent to be used is an extremely significant parameter depending on pollutant types in water and other affecting factors. The most extensively utilized adsorbent for water treatments has been activated carbons because of their considerable adsorption capabilities, various pore structures, alkali and acid resistance, great mechanical strength, and diverse functional groups on their surfaces [8, 11, 12]. To

✉ Ünal Geçgel
unalgecgel@trakya.edu.tr

[1] Food Science and Biotechnology, University for Business and Technology, Pristina, Kosova

[2] Arda Vocational College, Trakya University, Edirne 22030, Türkiye

[3] Department of Chemistry, Science and Art Faculty, Kırklareli University, Kırklareli 39020, Türkiye

fabricate low-cost activated carbons, agricultural biomass wastes, such as durian shell [13], fern leaves [14], sycamore balls, ripe black locust seed pods, *Nerium oleander* fruits [15], watermelon rind [16], tobacco stem [17], potato peels [18], almond shell [19], etc., have been used as raw materials in recent years. Usage of agricultural biomass wastes as raw materials in activated carbon productions provides recycling of waste material and economic advantages. Also, the contents of agricultural biomass wastes are hydrocarbons, carbohydrates, lipids, lignin, hemicelluloses, etc., comprising varied functional groups that will provide potentially high adsorption capacity of activated carbon to be produced [20].

Chemical activation using activation agents, such as alkalines, acids, and salts is a successful activation technique to enable improvement of micropore and mesopores, and considerably enhance the surface areas of carbon-based materials [21, 22]. Beside the types of precursors and activation agents, activation agent ratio, application method of activation agents, carbonization temperature, and carbonization duration are other significant factors influencing specific surface area and develop pore structure developments [23]. By considering these influencing factors, activated carbons have been obtained from various biomass waste precursors [24, 25].

In the literature review, Cafer Saka produced activated carbons from acorn shell collected from *Quercus petraea* usually renowned as sessile oak [26]. Compared to *Quercus petraea*, *Quercus cerris* L. (Turkey oak) native to most of western Asia and Europe is one of the different species of oak. Also, the different growth responses of these two species to drought conditions have been seen [27]. *Quercus cerris* L. is a large, deciduous broadleaf shade fast-growing tree, growing 40–60 feet tall. According to the literature review, it is determined that *Quercus cerris* acorn shell has not been used for activated carbon synthesis yet. For this reason, the aim of this study is to produce activated carbons from *Quercus cerris* acorn shell under various experiment conditions, and their characterizations were carried out by using Brunauer–Emmett–Teller (BET) specific surface areas, pore volumes, N_2 adsorption-desorption isotherms, pore distributions, Fourier Transform Infrared Spectroscopy (FTIR), Scanning Electron Microscope (SEM), elemental analyses, and Boehm titration.

2 Materials and methods

2.1 Materials

Quercus cerris acorn shells (starting material) were collected from an oak tree in Lokvica village (Zhupa region) located in Prizren city in Kosovo. Zinc chloride ($ZnCl_2$, CAS Number: 7646-85-7) was obtained from Merck. Hydrochloric acid (HCl, CAS Number: 7647-01-0), sodium bicarbonate ($NaHCO_3$, CAS Number: 144-55-8), sodium carbonate (Na_2CO_3, CAS Number: 497-19-8), and sodium hydroxide (NaOH, CAS Number: 1310-73-2) were purchased from Sigma-Aldrich. All chemical reagents utilized in this study were of analytical grade. The brand of porcelain crucibles and capsules used at the carbonization step was Haldenwenger.

2.2 Methods

After *Quercus cerris* acorn shells collected were washed with tap water and then distilled water to remove dirt, dust, and impurities, they were dried, ground, and sifted with a 50-mesh sieve. Similar method [16] was utilized to prepare activated carbons from acorn shells. The sieved acorn shell as the raw material of the activated carbon in this study was mixed with 80 mL $ZnCl_2$ solution prepared at various concentrations depending on $ZnCl_2$/raw material rates studied. For instance, 8 g acorn shell was treated with 80 mL aqueous solutions at various $ZnCl_2$ amounts of 8, 12, 16, and 20 g under reflux at boiling temperature for 5 h. After the reflux phase, the mixtures taken in the glass petri dishes were placed in an incubator (OF-02), and they were kept at 80 °C for 24 h. After that, the mixtures displaced in porcelain crucible were carbonized in a muffle furnace (Protherm furnaces) at various temperature values and carbonization times depending on the parameters to be examined. After carbonization, the activated carbons produced were allowed to cool down in a desiccator, washed with dilute HCL solution (0.5 N) and then distilled water to remove excess $ZnCl_2$ and impurities from activated carbon surfaces by using filter paper. Lastly, the activated carbons (QCACs) were dried at 70 °C in the incubator overnight, ground, and stored in glass bottles for their characterizations.

2.3 Characterization techniques of raw material and prepared activated carbons

Thermogravimetric analysis of raw material was completed by using an TGA analyzer (SETARAM instrumentation Labsys Evo). The TGA measurement temperature range was set from 30 to 1000 °C with 10 °C/min temperature increase and 20 mL/min N_2 flow. The yields of QCACs obtained were calculated by applying the formula given below.

$$Yield\,(\%) = \frac{W_A}{W_B} \times 100 \tag{1}$$

where, W_A (g) and W_B (g) represent the masses of activated carbon obtained and dried starting material, respectively.

BET surface area and porosity measurements of the resultant QCACs were carried out on an automatic apparatus (Micromeritics Gemini VII 2390t) using the BET method [28] by N_2 adsorption–desorption isotherms at temperature of liquid nitrogen (77 K) in the relative pressure (p/p_0) of 0.25. To eliminate volatile contaminations, the resultant activated carbons were held under N_2 atmosphere at 300 °C for 2 h before the BET measurements. Total pore volumes were calculated at relative pressure of 0.995, and t-Plot micropore volumes were obtained. Barrett–Joyner–Halenda (BJH) model [29] was utilized to find out pore size distributions. The mesopore volumes were computed by subtraction.

The functional groups on the surfaces of QCACs were studied by using Fourier Transform Infrared Spectroscopy (Perkin Elmer) and Boehm titration methods [30, 31]. According to Boehm titration, 1 g QCAC samples and Boehm reactants (0.1 N 100 mL NaOH, Na_2CO_3, and $NaHCO_3$) were shaken separately in 250 cm^3 Erlenmeyer Conical Flasks with Glass Stoppers for 24 h at 25 °C. The equilibrated Boehm reactants were filtrated from QCACs, and each 25.00 mL aliquot was pipetted to titrate the excess of base and acid with 0.1 N solutions of HCl or NaOH. The acidic site numbers of QCAC were determined under the assumption that $NaHCO_3$ neutralized just carboxylic acids, Na_2CO_3 neutralized carboxylic and lactonic, and NaOH neutralized carboxylic, lactonic, and phenolic groups. The basic site number of QCAC was computed from HCl amount reacted with QCAC. Furthermore, the image of sample was analyzed on scanning electron microscope (Zeiss Evo LS 10) to figure out their surface structure. Moreover, elemental compositions (C, H, N, S) of *Quercus cerris* acorn shell and QCACs were calculated by utilizing an elemental analyzer (Eager 300). Oxygen contents were computed by subtraction.

3 Results and discussion

3.1 Thermogravimetric analysis

TGA, dTG, and heat flow curves of *Quercus cerris* acorn shell to ascertain general decomposition characteristics during the activation and carbonization are given in Fig. 1. TG weight loss with 6.70% in the temperature range of 40–200 °C corresponds the dehydration and the existent of unstable cellulosic components on *Quercus cerris* acorn shell. The highest weight loses with 61.10% were determined between 200 and 670 °C, indicating that lignin, hemicellulose, and cellulose decomposed thermally [32]. Above 670 °C, weight loses with small amounts showed that the decomposition of some structure in *Quercus cerris* acorn shell still took place. The peak of heat flow curve at around 350 °C shows that the decomposition of *Quercus cerris* acorn shell is exothermic, while it is endothermic at around 750 °C. That is because cellulose, lignin, hemicellulose, and other volatile compounds may leave competitively from the structure

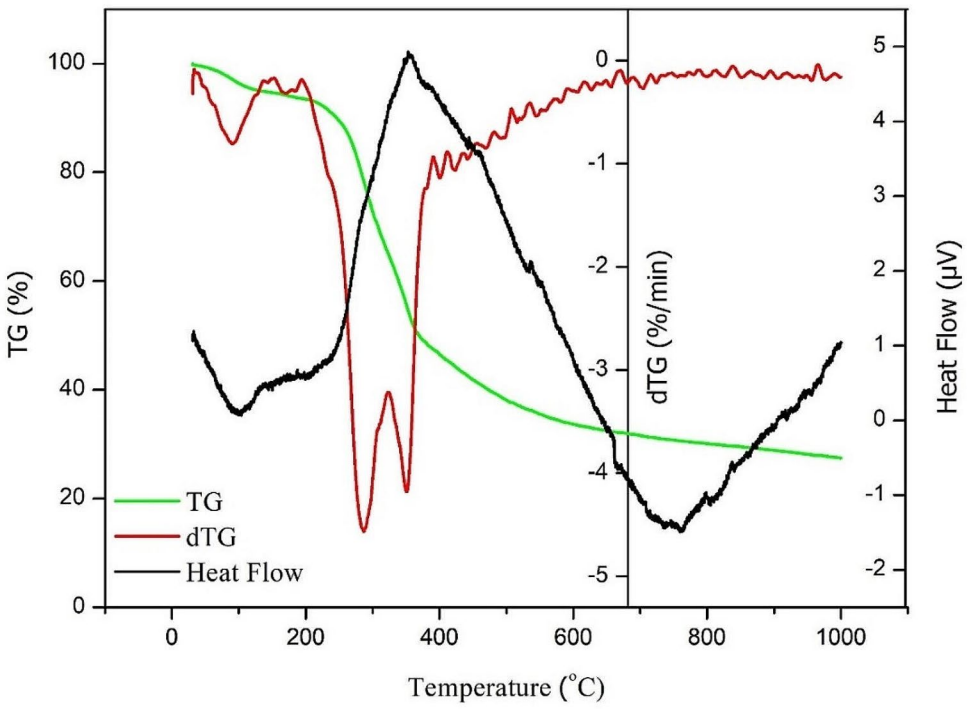

Fig. 1 TGA, dTG, and heat flow curves of *Quercus cerris* acorn shell

Table 1 Yields (%) of resultant activated carbons from *Quercus cerris* acorn shell at various production conditions

Constant parameters					
	Impregnation ratio ($ZnCl_2$/starting material, w/w)				
Carbonization temp. = 500 °C Carbonization time = 90 min.	1	1.5	2	2.5	
Yields	38.28	38.42	38.50	38.20	
	Temperature (°C)				
Impregnation ratio = 2/1 Carbonization time = 90 min.	400	500	600	700	800
Yields	40.30	38.50	36.4	34.10	31.60
	Carbonization time (min.)				
Impregnation ratio = 2/1 Carbonization temp. = 500 °C	60	90	120	150	180
Yields	39.20	38.50	37.80	36.55	35.75

dependent on temperature values, net energy changes, and thermodynamic properties.

3.2 Yields of activated carbons

Table 1 displays the yields of QCACs obtained from *Quercus cerris* acorn shell at various production conditions which are different carbonization temperature, carbonization time and impregnation ratio. When holding constant temperature at carbonization temperature of 500 °C for constant carbonization time of 90 min., a significant change over the yield of QCAC obtained with different impregnation ratios was not observed. The yield value was calculated around 38%. On the other hand, yield percentage decreased from 40.30 to 31.60 as carbonization temperature increased from 400 to 800 °C when using constant impregnation ratio of 2/1 for constant carbonization time of 90 min. Also, carbonization time showed negative effect on QCAC yields by decreasing yield from 39.20 to 35.75% when carbonization time increased. The reason for this decrease in QCAC yield can be explained with having more separation ability of volatile components from the structure when the carbonization temperature and time increase.

3.3 BET surface areas of QCACs

High surface area is one of the desired properties for adsorbents as it contributes positively to the adsorption capacity. To obtain an activated carbon with high surface area from *Quercus cerris* acorn shell, syntheses were performed under various conditions, and the results of their BET surface areas are presented in Fig. 2. One of the factors which affect surface area and other textural properties is impregnation ratio, therefore various impregnation ratios of $ZnCl_2$ were used to determine BET surface areas of QCAC at carbonization temperature of 500 °C for 90 min., as given in Fig. 2(a). As $ZnCl_2$/starting material ratio increased from 1.0 to 2.0, BET surface area of QCAC increased from 1356.36 to 1751.61 m^2/g. Nevertheless, BET surface area of QCAC decreased to 1630.23 m^2/g when the impregnation ratio was increased further to 2.5. Thus, the highest surface area of QCAC in experiments for impregnation ratio effect was obtained as

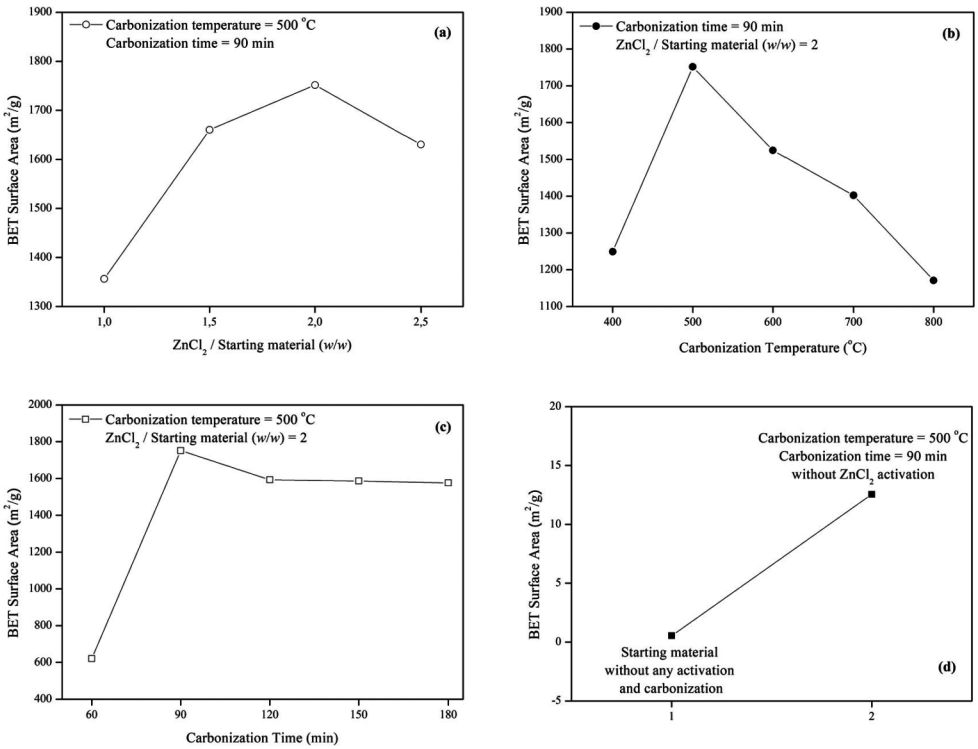

Fig. 2 BET surface areas of QCACs obtained by using (**a**) various $ZnCl_2$/starting material ratios at 500 °C for 90 min, (**b**) various carbonization temperatures for 90 min at constant $ZnCl_2$/starting material ratios value of 2/1, (**c**) various carbonization times at constant carbonization temperature of 500 °C and constant $ZnCl_2$/starting material ratios value of 2/1, and (**d**) starting material and activated carbon obtained without $ZnCl_2$ activation

1751.61 m^2/g when used at the impregnation ratio of 2.0 at 500 °C for 90 min.

One of the other factors affecting surface area is carbonization temperature due to the needed energy absorbed or released for the interaction of the starting material with $ZnCl_2$ and the release of volatile groups during the carbonization. Figure 2(b) displays BET surface areas of QCAC when synthesized by using constant impregnation ratio of 2.0 at various carbonization temperatures for 90 min. When carbonization temperature increased from 400 to 500 °C, BET surface area of QCAC increased from 1249.16 to 1751.61 m^2/g. On the other hand, BET surface area of QCAC decreased from 1751.61 to 1170.82 m^2/g as carbonization temperature increased from 500 to 800 °C. Hence, the optimum carbonization temperature in experiments for carbonization temperature effect was determined as 500 °C when used constant impregnation ratio of 2.0 for carbonization time of 90 min.

Carbonization time is also a significant factor, so QCACs were produced at various carbonization times by holding following parameters constant; carbonization temperature of 500 °C and impregnation ratio of 2, and their BET surface area results are presented in Fig. 2(c). When carbonization time increased from 60 to 90 min., BET surface area of QCAC increased from 620.64 to 1751.61 m^2/g. This can be explained by the need for sufficient time for the interaction of $ZnCl_2$ and the starting material, and it seems that the carbonization time of 60 min. is not sufficient under these conditions. When carbonization time was increased further from 90 to 180 min., BET surface area of QCAC declined from 1751.61 to 1576.39 m^2/g. Also, BET surface areas of the starting material and the activated carbon obtained without $ZnCl_2$ activation were presented in Fig. 2(d) to determine whether $ZnCl_2$ influences surface area. BET surface areas of the starting material and the activated carbon obtained without $ZnCl_2$ usage was measured as 0.54 and 12.55 m^2/g, respectively. Overall, in the experiments conducted, the highest surface area of QCAC was determined to be 1751.61 m^2/g when utilized at the impregnation ratio of 2.0 at 500 °C for 90 min.

3.4 Pore volumes and pore size distributions of QCACs

It is a desirable feature for activated carbon to be enhanced porosity, as it provides its usability as an adsorbent for the adsorption of various substances. While mesoporosity size is significant in the adsorption of liquid phase pollutants, high microporous activated carbons are selected in gas and storage applications [33]. Also, highly mesoporosity is favorable at the adsorptions of metal and organic dye [34]. $ZnCl_2$ is a Lewis acid, has a dehydrating function in activated carbon productions and does not react with carbon, therefore it is used to form an activated carbon with higher porosity and surface area [25]. To examine the pore structure of QCAC, Fig. 3 displays the pore volumes of QCAC

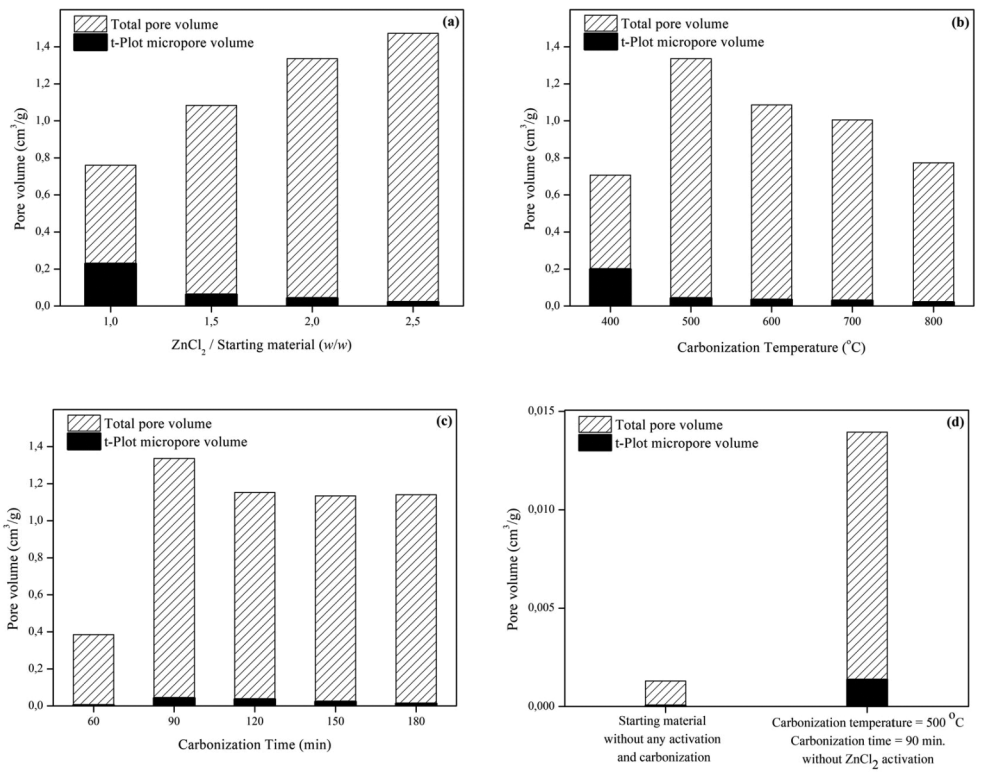

Fig. 3 Pore volumes of QCACs obtained by utilizing (**a**) various $ZnCl_2$/starting material ratios at 500 °C for 90 min, (**b**) various carbonization temperatures for 90 min at constant $ZnCl_2$/starting material ratio value of 2/1, (**c**) various carbonization times at constant carbonization temperature of 500 °C and constant $ZnCl_2$/starting material ratio value of 2/1, and (**d**) starting material and activated carbon obtained from carbonization without $ZnCl_2$

produced under various experiment conditions. When impregnation ratio was increased from 1.0 to 2.5, the total pore volume of QCAC increased from 0.761 to 1.473 cm^3/g, but the micropore volume of QCAC decreased from 0.228 to 0.022 cm^3/g, as seen in Fig. 3(a). Moreover, the mesopore volume of QCAC increased from 0.533 to 1.451 cm^3/g, as impregnation ratio was increased from 1.0 to 2.5. When low $ZnCl_2$ ratios are used, $ZnCl_2$ acts as a dehydration agent, causing micropore formation and expansion, while when high $ZnCl_2$ ratio is used, some amount of $ZnCl_2$ remains on the outside of the starting material and decomposes the organic compounds, resulting in the formation of more mesopores and macropores [35].

Using the constant impregnation ratio of 2.0 and the constant carbonization period of 90 min, as seen in Fig. 3(b), the total pore volume (0.707 cm^3/g) of QCAC produced at 400 °C is lower than that (1.336 cm^3/g) produced at 500 °C, but the micropore volume (0.199 cm^3/g) produced at 400 °C is higher than that (0.042 cm^3/g) at 500 °C. This may be explained that higher thermal energy makes more active $ZnCl_2$ to expand pore volume. On the contrary, the total pore and the micropore volumes of QCAC reduced from 1.336 to 0.774 cm^3/g, and from 0.042 to 0.021 cm^3/g, respectively, when carbonization temperature increased from 500 to 800 °C. This phenomenon is caused by the sintering effect of volatile compounds and carbon structure shrinking at higher temperatures, leading to pore contraction and closure [36].

Carbonization period is also another significant parameter affecting pore volume, and the results are given in Fig. 3(c). By using the constant impregnation ratio of 2.0 and the constant carbonization temperature of 500 °C, the total pore and micropore volumes of QCAC increased from 0.385 to 1.336 cm^3/g and from 0.004 to 0.042 cm^3/g, respectively, when carbonization time was altered from 60 to 90 min. On the other hand, the total pore and micropore volumes of QCAC increased from 1.336 to 1.141 cm^3/g and from 0.042 to 0.013 cm^3/g, respectively, when carbonization time was increased from 90 to 180 min. Moreover, the pore volumes of the starting material and activated carbon produced from carbonization without activation agent are given in Fig. 3(d). The total pore and micropore volumes of the starting material were determined to be 0.001 and almost 0 cm^3/g, respectively. The total pore and micropore volumes of the activated carbon produced without $ZnCl_2$ were found 0.014 and 0.001 cm^3/g, respectively. These findings proved that $ZnCl_2$ was a significant activating agent in terms of obtaining QCAC with high porosity.

When a high adsorption capacity or a productive adsorption process are desired, pore size distribution provides significant information to choose an adsorbent with an appropriate pore size to the adsorbate size. As shown in Fig. 4 presenting pore distributions of QCACs produced, the pore sizes of QCACs were mostly mesopores. It is seen from Fig. 4(a) that the high incremental pore volume values of QCACs are in the range 2 to 10 nm pore width. In this range, the highest incremental pore volume value of QCAC was determined when utilized the impregnation ratio of 2.5/1. Likewise, high incremental pore volume values of

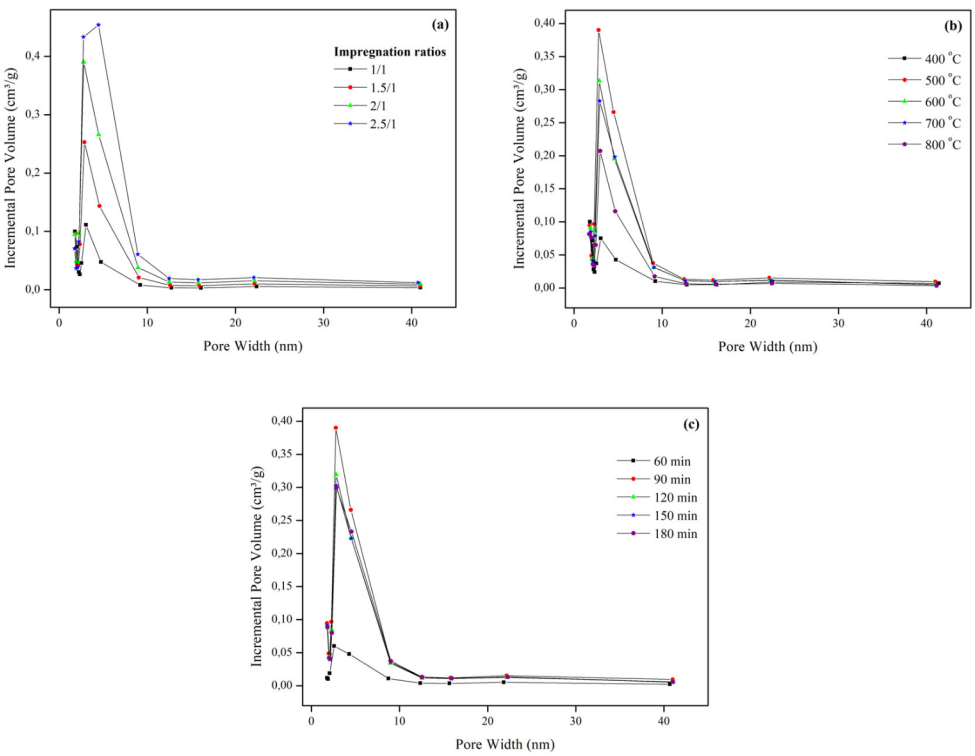

Fig. 4 Pore distributions of QCACs obtained by using (**a**) various $ZnCl_2$/starting material ratios at 500 °C for 90 min, (**b**) various carbonization temperatures for 90 min at constant $ZnCl_2$/starting material ratio value of 2/1, and (**c**) various carbonization times at constant carbonization temperature of 500 °C and constant $ZnCl_2$/starting material ratio value of 2/1

QCACs were found out in the range 2 to 10 nm pore width, as presented in Fig. 4(b-c). From the pore distribution data, it was determined that QCACs had mainly narrow mesopores and a very little amount of micropores.

3.5 N_2 adsorption–desorption isotherms

The isotherms in Fig. 5 at a relative pressure of $0-0.1$ exhibit N_2 adsorption-desorption isotherm plots of QCACs achieved under various experiment conditions. According to the International Union of Pure and Applied Chemistry (IUPAC), physisorption isotherms were categorized with six different types [37], and it was developed in later years [38]. The first nitrogen uptake was important in the low-pressure region where $p/p_0 < 0.1$, and the second knee formed in the range of $p/p_0 > 0.8$ for almost all isotherm plots as shown in Fig. 5(a), which specifying the appearance of pore widening process and the mesoporosity improvement [35]. When impregnation ratio was increased from 1.0 to 2.5, the isotherms of QCACs turned into more like type IV(a) from type I. Also, their hysteresis loops resembled H4 type proposing the presence of narrow slit-shaped pores in QCACs [37]. The hysteresis loops enlarged with increasing impregnation ratio, proving more mesopore formation, is also in accordance with the pore volume results because pore volume reduced with increasing impregnation ratio. The hysteresis loops of Type IV isotherms of QCACs are related to capillary condensation become in mesopores and the restricting uptake at high $p/p°$ values, and the first stage of Type IV isotherms was due to monolayer-multilayer adsorption [37].

Like the results obtained from impregnation ratio effect, the isotherm types of QCACs were determined to resemble Type IV and H4 hysteresis type from the results from the effects of carbonization temperature and carbonization period, as seen in Fig. 5(b-c). When carbonization temperature was increased from 400 to 500 °C, N_2 adsorption quantity of QCAC increased. However, N_2 adsorption quantity of QCAC reduced when carbonization temperature was reduced from 500 to 800 °C. These results are compatible with the pore volume results since the highest total volume were determined for QCAC produced at carbonization temperature of 500 °C. Moreover, N_2 adsorption quantity of QCAC increased when used carbonization period was increased from 60 to 90 min. When increasing carbonization period to higher than 90 min., it was determined that N_2 adsorption quantity of QCAC reduced and did not change much with even more increasing carbonization time. Thus, it was understood that QCACs produced under various conditions mostly had mesopore structures and their pores were narrow slit-shaped.

3.6 Functional groups of QCAC by FTIR spectra and Boehm titration

The FT-IR spectra of QCAC and starting material in Fig. 6 were obtained to figure out their surface groups. At the FT-IR spectrum of starting material, the broad absorption

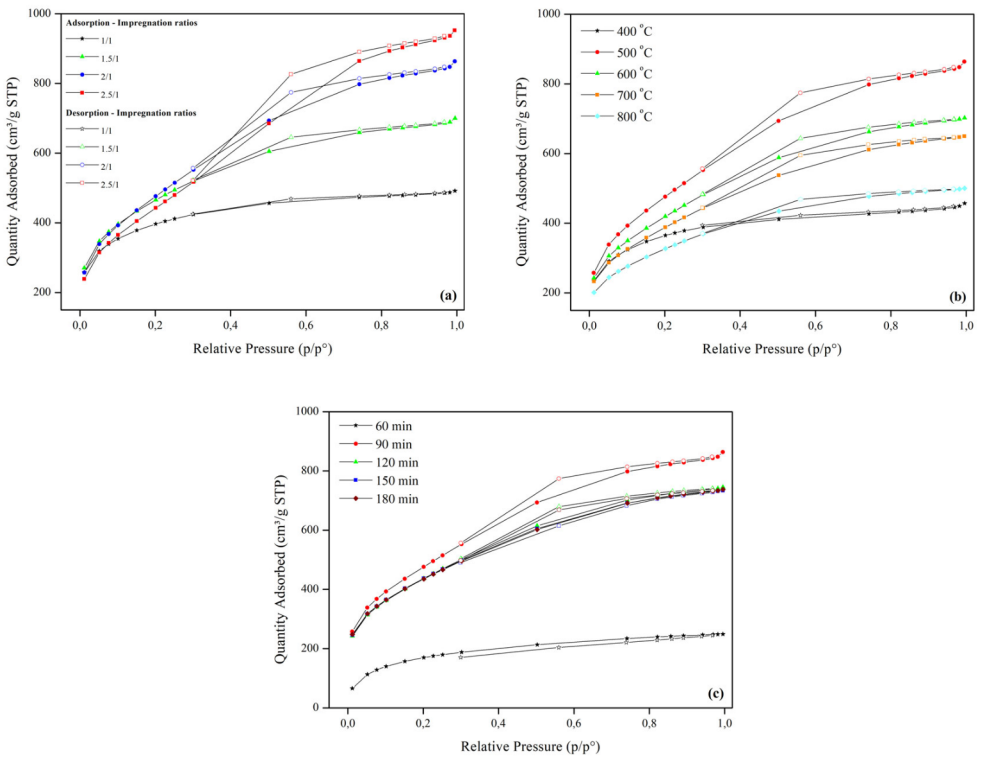

Fig. 5 N_2 adsorption-desorption isotherm plots of QCACs produced by using (**a**) various $ZnCl_2$/ starting material ratios at 500 °C for 90 min, (**b**) various carbonization temperatures for 90 min at constant $ZnCl_2$/ starting material ratio value of 2/1, and (**c**) various carbonization times at constant carbonization temperature of 500 °C and constant $ZnCl_2$/ starting material ratio value of 2/1

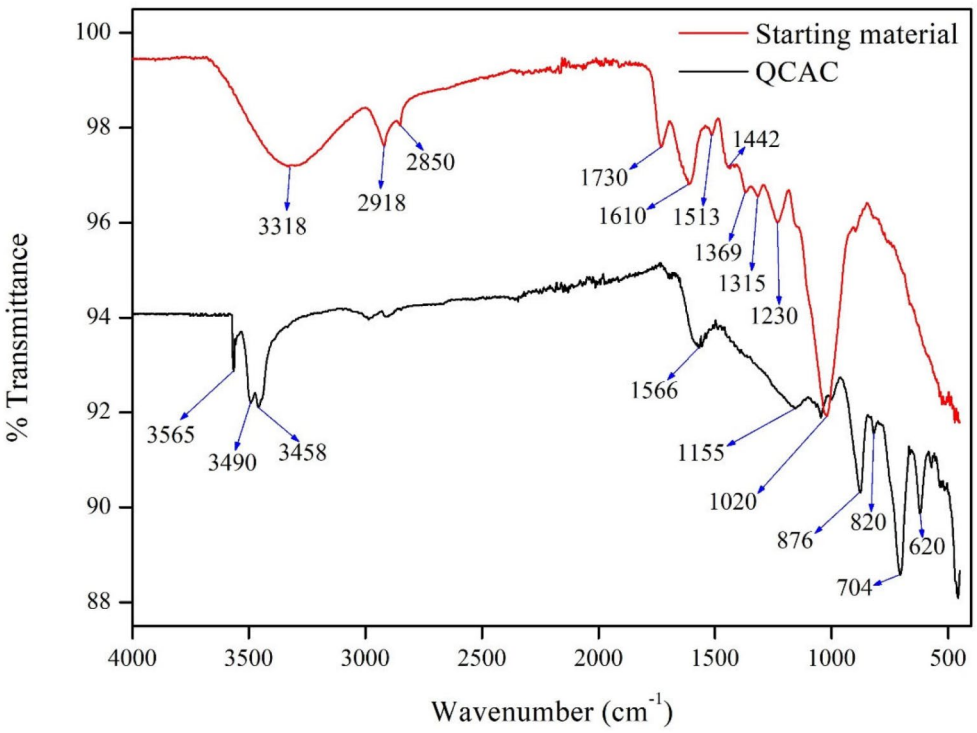

Fig. 6 FT-IR spectra of QCAC and starting material

Table 2 Results of Boehm titration (meq/g)

Activated carbon	Acidic groups			Acidic (total)	Basic (total)	All groups (total)
	Carboxyl	Phenolic	Lactonic			
QCAC	0.05	0.50	0.37	0.92	0.58	1.50

peak at 3318 cm^{-1} corresponds to O–H stretching vibrations of absorbed water and hydroxyl groups present in starting material, such as alcohols, phenols, and carboxylic groups [39]. The two peaks appearing at 2918 and 2850 cm^{-1} are assigned to symmetric and asymmetric stretching C–H vibrations, respectively, in the methyl, methylene, and aromatic methoxy groups [40, 41]. The peak located at 1730 cm^{-1} can be due to the C–O stretching and C = O stretching vibrations arising from carbonyl, ester, and ketone groups [39, 40, 42]. The peaks corresponded to the C = C stretching vibrations of aromatic rings are observed at 1610, 1513, and 1442 cm^{-1} [40, 43, 44]. The peak at 1369 cm^{-1} can be ascribed to C–H deformation in hemicellulose and cellulose or the C–N groups of aliphatic and aromatic amines [45, 46]. The peak at 1315 cm^{-1} may be assigned to C–H wagging or phenolic hydroxyl (Ar)O–H [47, 48]. C–O stretching vibrations are observed at 1230 and 1020 cm^{-1} [39, 49, 50]. As for the spectrum of QCAC, the peaks at 3565, 3490 and 3458 cm^{-1} reveal –OH stretching vibrations due to hydroxyl groups and weakly bound absorbed water [51–53]. The band at around 1566 cm^{-1} is ascribed to C–C vibration in aromatics groups [54, 55]. The peak at 1155 cm^{-1} reveals the presence of C–O vibration [56]. The peaks at 876 and 820 cm^{-1} are because of the C–H stretching vibrations in aromatic groups [57, 58]. Also, the peaks between 750 and 500 cm^{-1} could be due to C–C stretching and C–H bending [59, 60]. Furthermore, the results of Boehm titration experiments are displayed in Table 2. It is seen that QCAC contains acidic groups as the highest content, almost two times to the basic groups. Among these acidic groups, phenolic groups are the most abundant.

3.7 Textural characterization by SEM

The SEM image of the activated carbon with highest surface area was obtained by utilizing scanning electron microscopy to examine the surface morphology of the sample. Figure 7 presents the SEM image of QCAC produced by using impregnation ratio of 2.0 at carbonization temperature of 500 °C for carbonization time of 90 min. It is seen that QCAC is a highly porous material with various cracks, voids, large holes, and channels on the surface of QCAC.

3.8 Elemental analyses

The elemental analysis results (N, C, H, S, and O contents) of QCAC prepared from *Quercus cerris* acorn shells at

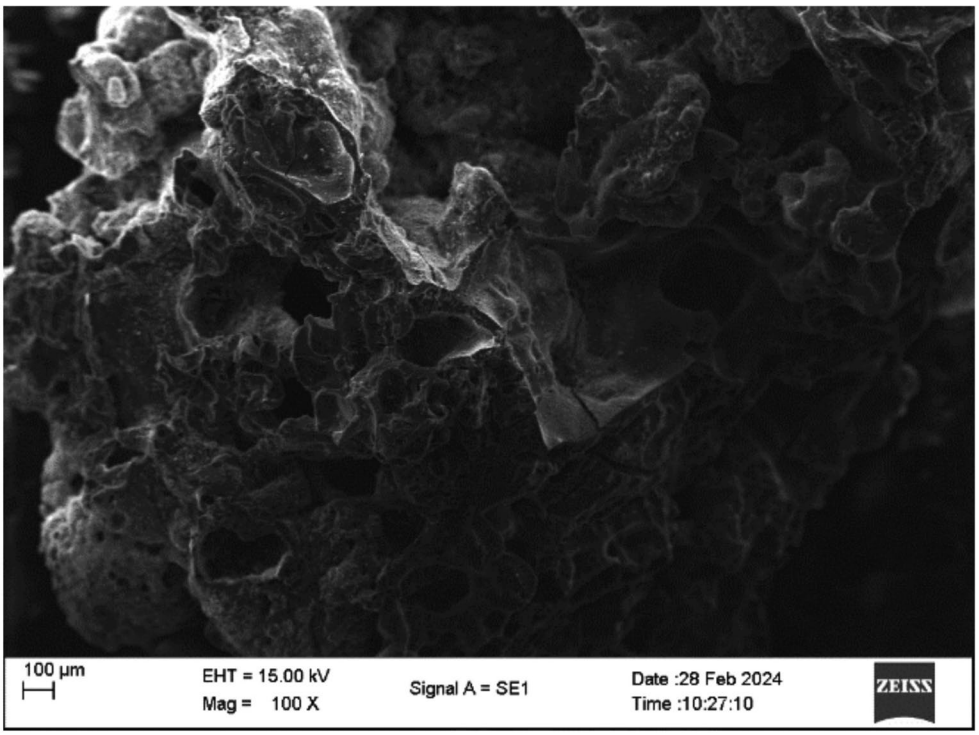

Fig. 7 SEM image of QCAC obtained by using impregnation ratio of 2.0 at carbonization temperature of 500 °C for carbonization time of 90 min

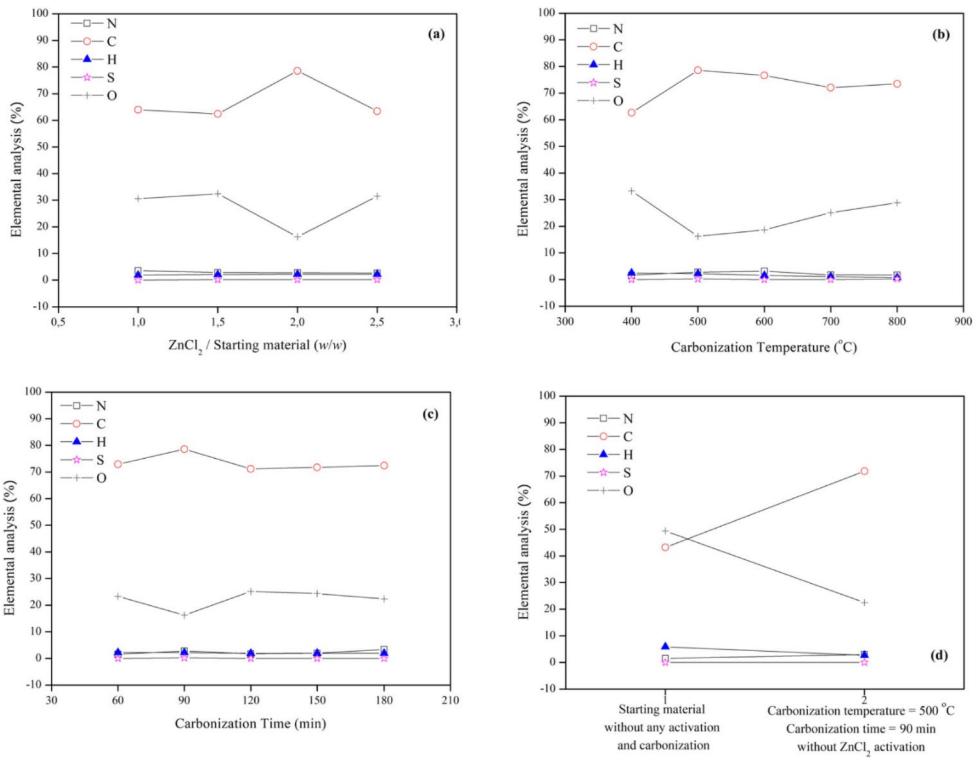

Fig. 8 Elemental analysis results of QCAC synthesized by using (**a**) various $ZnCl_2$/starting material ratios at 500 °C for 90 min, (**b**) various carbonization temperatures for 90 min at constant $ZnCl_2$/starting material ratios value of 2/1, (**c**) various carbonization times at constant carbonization temperature of 500 °C and constant $ZnCl_2$/starting material ratios value of 2/1, and (**d**) starting material and activated carbon produced without $ZnCl_2$ activation

various impregnation ratios under various carbonization circumstances were showed in Fig. 8. The nitrogen content of the produced activated carbons changed between 1.64% and 3.56%, the carbon content changed between 62.66% and 78.58%, the hydrogen content was between 0.71% and 2.45%, the sulfur content was between 0% and 0.26% and the oxygen content varied between 16.23% and 33.24%. The highest carbon content (78.58%) of QCAC was obtained by using $ZnCl_2$/starting material ratio of 2.0 at 500 °C for 90 min. Moreover, as given in Fig. 8(d), the carbon content of QCAC produced without $ZnCl_2$ activation was 71.84%,

while the carbon content of starting material without any activation and carbonization was determined to be 43.20%.

4 Conclusions

Preparation and characterization of activated carbons obtained from *Quercus cerris* acorn shells with $ZnCl_2$ chemical activation by using various production conditions were demonstrated in this study. The influence of carbonization temperatures (400–800 °C), carbonization period (60–180 min.) and impregnation ratios (1.0–2.0) on the activated carbon yields, surface areas, pore developments, and N_2 adsorption–desorption isotherms were examined. The QCAC yields reduced with increasing carbonization temperature and carbonization period. The highest surface area of QCAC was determined to be 1751.61 m^2/g when utilized at the impregnation ratio of 2.0 at 500 °C for 90 min. The carbonization temperature, carbonization period, and impregnation ratio had an important effect on the pore characteristic developments of QCAC. When impregnation ratio was increased, the total pore volume of QCAC increased, but the micropore volume of QCAC decreased. The pore distribution data showed that QCACs had mainly narrow mesopores and a little amount of micropores. From the N_2 adsorption–desorption isotherm data, QCACs obtained under various conditions mostly had mesopore structures and their pores were determined to be narrow slit-shaped. Also, the data obtained from FTIR, Boehm titration, SEM, and elemental analysis provided more information about QCACs produced. *Quercus cerris* acorn shells can be effectively utilized as a starting material for activated carbon preparation by $ZnCl_2$ chemical activation, and the resultant activated carbons might be utilized for efficiently wastewater treatments. For this reason, our next work will be to test the adsorption performance of QCACs towards impurities in aqueous solutions.

Acknowledgements We would like to thank the Ministry of Education, Science and Technology of Kosovo for financially supporting our project under the project number of 2-2541-1 in 2023; whose project title is "Largimi i ndotësve nga sinteza e karbonit të aktivizuar nga biomaterialet e mbeturinave bujqësore dhe procesi i absorbimit nga ujërat e zeza".

Author contributions C.Ç.: Conceptualization, Methodology, Validation, Formal analysis, Investigation, Resources, Writing - Original Draft, Writing - Review & Editing, Supervision, Project administration, Funding acquisition. Ü.G.: Methodology, Formal analysis, Writing - Original Draft, Writing - Review & Editing. H.K.: Conceptualization, Methodology, Validation, Investigation. O.Ü.: Methodology, Formal analysis, Writing - Original Draft, Writing - Review & Editing. D.N.: Validation, Investigation. Berat Durmishi: Validation, Investigation. R.D.: Validation, Investigation. Diellëza Elshani: Conceptualization, Methodology, Validation, Investigation. H.P.: Formal analysis. All authors have read, reviewed, and agreed to publish this version of the manuscript.

Funding Open access funding provided by the Scientific and Technological Research Council of Türkiye (TÜBİTAK). This work was supported by the Ministry of Education, Science and Technology of Kosovo under the project number of 2-2541-1 in 2023.
Open access funding provided by the Scientific and Technological Research Council of Türkiye (TÜBİTAK).

Data availability No datasets were generated or analysed during the current study.

Declarations

Ethical approval This is not applicable in this article.

Competing interests The authors declare no competing interests.

References

1. Piriya, R.S., Jayabalakrishnan, R.M., Maheswari, M., Boomiraj, K., Oumabady, S.: Comparative adsorption study of malachite green dye on acid-activated carbon. J. Environ. Anal. Chem. **103**(1), 16–30 (2023). https://doi.org/10.1080/03067319.2020.1849667
2. Dutta, A.K., Maji, S.K., Adhikary, B.: γ-Fe2O3 nanoparticles: An easily recoverable effective photo-catalyst for the degradation of rose bengal and methylene blue dyes in the waste-water treatment plant. Mater. Res. Bull. **49**, 28–34 (2014). https://doi.org/10.1016/j.materresbull.2013.08.024
3. Morin-Crini, N., Lichtfouse, E., Liu, G., Balaram, V., Ribeiro, A.R.L., Lu, Z., Stock, F., Carmona, E., Teixeira, M.R., Picos-Corrales, L.A., Moreno-Piraján, J.C., Giraldo, L., Li, C., Pandey, A., Hocquet, D., Torri, G., Crini, G.: Worldwide cases of water pollution by emerging contaminants: A review. Environ. Chem. Lett. **20**(4), 2311–2338 (2022). https://doi.org/10.1007/s10311-022-01447-4
4. Zamora-Ledezma, C., Negrete-Bolagay, D., Figueroa, F., Zamora-Ledezma, E., Ni, M., Alexis, F., Guerrero, V.H.: Heavy metal water pollution: A fresh look about hazards, novel and conventional remediation methods. Environ. Technol. Innov. **22**, 101504 (2021). https://doi.org/10.1016/j.eti.2021.101504
5. Gan, Y., Ding, C., Xu, B., Liu, Z., Zhang, S., Cui, Y., Wu, B., Huang, W., Song, X.: Antimony (Sb) pollution control by coagulation and membrane filtration in water/wastewater treatment: A comprehensive review. J. Hazard. Mater. **442**, 130072 (2023). https://doi.org/10.1016/j.jhazmat.2022.130072
6. Saleh, T.A., Mustaqeem, M., Khaled, M.: Water treatment technologies in removing heavy metal ions from wastewater: A

review. Environ. Nanotechnol Monit. Manag. **17**, 100617 (2022). https://doi.org/10.1016/j.enmm.2021.100617
7. Bal, G., Thakur, A.: Distinct approaches of removal of dyes from wastewater: A review. Mater. Today Proc. **50**, 1575–1579 (2022). https://doi.org/10.1016/j.matpr.2021.09.119
8. Mousavi, S.A., Kamarehie, B., Almasi, A., Darvishmotevalli, M., Salari, M., Moradnia, M., Azimi, F., Ghaderpoori, M., Neyazi, Z., Karami, M.A.: Removal of rhodamine B from aqueous solution by stalk corn activated carbon: Adsorption and kinetic study. Biomass Convers. Biorefin. **13**(9), 7927–7936 (2023). https://doi.org/10.1007/s13399-021-01628-1
9. Rashid, R., Shafiq, I., Akhter, P., Iqbal, M.J., Hussain, M.: A state-of-the-art review on wastewater treatment techniques: The effectiveness of adsorption method. Environ. Sci. Pollut Res. **28**, 9050–9066 (2021). https://doi.org/10.1007/s11356-021-12395-x
10. De Gisi, S., Lofrano, G., Grassi, M., Notarnicola, M.: Characteristics and adsorption capacities of low-cost sorbents for wastewater treatment: A review. Sustain. Mater. Technol. **9**, 10–40 (2016). https://doi.org/10.1016/j.susmat.2016.06.002
11. Wang, X., Cheng, H., Ye, G., Fan, J., Yao, F., Wang, Y., Jiao, Y., Zhu, W., Huang, H., Ye, D.: Key factors and primary modification methods of activated carbon and their application in adsorption of carbon-based gases: A review. Chemosphere. **287**, 131995 (2022). https://doi.org/10.1016/j.chemosphere.2021.131995
12. Jawad, A.H., Abdulhameed, A.S., Wilson, L.D., Syed-Hassan, S.S.A., ALOthman, Z.A., Khan, M.R.: High surface area and mesoporous activated carbon from KOH-activated dragon fruit peels for methylene blue dye adsorption: Optimization and mechanism study. Chin. J. Chem. Eng. **32**, 281–290 (2021). https://doi.org/10.1016/j.cjche.2020.09.070
13. Roddaeng, S., Promvonge, P., Anuwattana, R., Vongpanit, P., Suriyachai, N., Imman, S., Kreetachat, T., Kreetachat, N.: Synthesis of durian shell activated carbon by KOH activation using response surface methodology: Characterization and optimization of process parameters. Emerg. Mater. 1–13 (2024). https://doi.org/10.1007/s42247-024-00641-0
14. Serafin, J., Dziejarski, B., Vendrell, X., Kiełbasa, K., Michalkiewicz, B.: Biomass waste fern leaves as a material for a sustainable method of activated carbon production for CO2 capture. Biomass Bioenergy. **175**, 106880 (2023). https://doi.org/10.1016/j.biombioe.2023.106880
15. Üner, O., Geçgel, Ü., Avcu, T.: Comparisons of activated carbons produced from sycamore balls, ripe black Locust seed pods, and Nerium oleander fruits and also their H2 storage studies. Carbon Lett. **31**(1), 75–92 (2021). https://doi.org/10.1007/s42823-020-00151-z
16. Üner, O., Geçgel, Ü., Bayrak, Y.: Preparation and characterization of mesoporous activated carbons from waste watermelon rind by using the chemical activation method with zinc chloride. Arab. J. Chem. **12**(8), 3621–3627 (2019). https://doi.org/10.1016/j.arabjc.2015.12.004
17. Chen, R., Li, L., Liu, Z., Lu, M., Wang, C., Li, H., Ma, W., Wang, S.: Preparation and characterization of activated carbons from tobacco stem by chemical activation. J. Air Waste Manag Assoc. **67**(6), 713–724 (2017). https://doi.org/10.1080/10962247.2017.1280560
18. Kyzas, G.Z., Deliyanni, E.A., Matis, K.A.: Activated carbons produced by pyrolysis of waste potato peels: Cobalt ions removal by adsorption. Colloids Surf. A: Physicochem Eng. Asp. **490**, 74–83 (2016). https://doi.org/10.1016/j.colsurfa.2015.11.038
19. Izquierdo, M.T., de Yuso, A.M., Rubio, B., Pino, M.R.: Conversion of almond shell to activated carbons: Methodical study of the chemical activation based on an experimental design and relationship with their characteristics. Biomass Bioenergy. **35**(3), 1235–1244 (2011). https://doi.org/10.1016/j.biombioe.2010.12.016
20. Shukla, S.K., Al Mushaiqri, N.R.S., Al Subhi, H.M., Yoo, K., Sadeq, A.: Low-cost activated carbon production from organic waste and its utilization for wastewater treatment. Appl. Water Sci. **10**(2), 62 (2020). https://doi.org/10.1007/s13201-020-1145-z
21. Singh, G., Ruban, A.M., Geng, X., Vinu, A.: Recognizing the potential of K-salts, apart from KOH, for generating porous carbons using chemical activation. Chem. Eng. J. **451**, 139045 (2023). https://doi.org/10.1016/j.cej.2022.139045
22. Wu, H.Y., Chen, S.S., Liao, W., Wang, W., Jang, M.F., Chen, W.H., Ahamad, T., Alshehri, S.M., Hou, C.H., Lin, K.S., Charinpanitkul, T., Wu, K.C.W.: Assessment of agricultural waste-derived activated carbon in multiple applications. Environ. Res. **191**, 110176 (2020). https://doi.org/10.1016/j.envres.2020.110176
23. Amin, M., Chung, E., Shah, H.H.: Effect of different activation agents for activated carbon preparation through characterization and life cycle assessment. Int. J. Environ. Sci. Technol. **20**, 7645–7656 (2023). https://doi.org/10.1007/s13762-022-04472-6
24. Gayathiri, M., Pulingam, T., Lee, K.T., Sudesh, K.: Activated carbon from biomass waste precursors: Factors affecting production and adsorption mechanism. Chemosphere. **294**, 133764 (2022). https://doi.org/10.1016/j.chemosphere.2022.133764
25. Jjagwe, J., Olupot, P.W., Menya, E., Kalibbala, H.M.: Synthesis and application of granular activated carbon from biomass waste materials for water treatment: A review. J. Bioresour Bioprod. **6**(4), 292–322 (2021). https://doi.org/10.1016/j.jobab.2021.03.003
26. Saka, C.: BET, TG–DTG, FT-IR, SEM, iodine number analysis and preparation of activated carbon from acorn shell by chemical activation with ZnCl2. J. Anal. Appl. Pyrol. **95**, 21–24 (2012). https://doi.org/10.1016/j.jaap.2011.12.020
27. Móricz, N., Illés, G., Mészáros, I., Garamszegi, B., Berki, I., Bakacsi, Z., Kámpel, J., Szabó, O., Rasztovits, E., Cseke, K., Bereczki, K., Németh, T.M.: Different drought sensitivity traits of young sessile oak (Quercus petraea (Matt.) Liebl.) And Turkey oak (Quercus cerris L.) stands along a precipitation gradient in Hungary. Ecol. Manag. **492**, 119165 (2021). https://doi.org/10.1016/j.foreco.2021.119165
28. Brunauer, S., Emmett, P.H., Teller, E.: Adsorption of gases in multimolecular layers. J. Am. Chem. Soc. **60**(2), 309–319 (1938). https://doi.org/10.1021/ja01269a023
29. Barrett, E.P., Joyner, L.G., Halenda, P.P.: The determination of pore volume and area distributions in porous substances. I. computations from nitrogen isotherms. J. Am. Chem. Soc. **73**(1), 373–380 (1951). https://doi.org/10.1021/ja01145a126
30. Boehm, H.P.: Some aspects of the surface chemistry of carbon blacks and other carbons. Carbon. **32**(5), 759–769 (1994). https://doi.org/10.1016/0008-6223(94)90031-0
31. Boehm, H.P.: Surface oxides on carbon and their analysis: A critical assessment. Carbon. **40**(2), 145–149 (2002). https://doi.org/10.1016/S0008-6223(01)00165-8
32. Ozdemir, I., Şahin, M., Orhan, R., Erdem, M.: Preparation and characterization of activated carbon from grape stalk by zinc chloride activation. Fuel Process. Technol. **125**, 200–206 (2014). https://doi.org/10.1016/j.fuproc.2014.04.002
33. Mak, S.M., Tey, B.T., Cheah, K.Y., Siew, W.L., Tan, K.K.: Porosity characteristics and pore developments of various particle sizes palm kernel shells activated carbon (PKSAC) and its potential applications. Adsorption. **15**, 507–519 (2009). https://doi.org/10.1007/s10450-009-9201-x
34. Jones, I., Zhu, M., Zhang, J., Zhang, Z., Preciado-Hernandez, J., Gao, J., Zhang, D.: The application of spent tyre activated carbons as low-cost environmental pollution adsorbents: A technical review. J. Clean. Prod. **312**, 127566 (2021). https://doi.org/10.1016/j.jclepro.2021.127566
35. Lu, X., Jiang, J., Sun, K., Xie, X.: Preparation and characterization of sisal fiber-based activated carbon by chemical activation

with zinc chloride. Bull. Korean Chem. Soc. **35**(1), 103–110 (2014). https://doi.org/10.5012/bkcs.2014.35.1.103
36. Lua, A.C., Yang, T.: Characteristics of activated carbon prepared from pistachio-nut shell by zinc chloride activation under nitrogen and vacuum conditions. J. Colloid Interface Sci. **290**(2), 505–513 (2005). https://doi.org/10.1016/j.jcis.2005.04.063
37. Sing, K.S.: Reporting physisorption data for gas/solid systems with special reference to the determination of surface area and porosity (recommendations 1984). Pure Appl. Chem. **57**(4), 603–619 (1985). https://doi.org/10.1351/pac198557040603
38. Thommes, M., Kaneko, K., Neimark, A.V., Olivier, J.P., Rodriguez-Reinoso, F., Rouquerol, J., Sing, K.S.: Physisorption of gases, with special reference to the evaluation of surface area and pore size distribution (IUPAC Technical Report). Pure Appl. Chem. **87**(9–10), 1051–1069 (2015). https://doi.org/10.1515/pac-2014-1117
39. Gundogdu, A., Duran, C., Senturk, H.B., Soylak, M., Imamoglu, M., Onal, Y.: Physicochemical characteristics of a novel activated carbon produced from tea industry waste. J. Anal. Appl. Pyrol. **104**, 249–259 (2013). https://doi.org/10.1016/j.jaap.2013.07.008
40. Salim, R.M., Asik, J., Sarjadi, M.S.: Chemical functional groups of extractives, cellulose and lignin extracted from native Leucaena leucocephala bark. Wood Sci. Technol. **55**, 295–313 (2021). https://doi.org/10.1007/s00226-020-01258-2
41. Sayğılı, H., Güzel, F.: High surface area mesoporous activated carbon from tomato processing solid waste by zinc chloride activation: Process optimization, characterization and dyes adsorption. J. Clean. Prod. **113**, 995–1004 (2016). https://doi.org/10.1016/j.jclepro.2015.12.055
42. Kanjana, K., Harding, P., Kwamman, T., Kingkam, W., Chutimasakul, T.: Biomass-derived activated carbons with extremely narrow pore size distribution via eco-friendly synthesis for supercapacitor application. Biomass Bioenergy. **153**, 106206 (2021). https://doi.org/10.1016/j.biombioe.2021.106206
43. Poto, S., Aguirre, A., Huigh, F., Llosa-Tanco, M.A., Pacheco-Tanaka, D.A., Gallucci, F., d'Angelo, M.F.N.: Carbon molecular sieve membranes for water separation in CO2 hydrogenation reactions: Effect of the carbonization temperature. J. Membr. Sci. **677**, 121613 (2023). https://doi.org/10.1016/j.memsci.2023.121613
44. Meng, F., Yu, J., Tahmasebi, A., Han, Y., Zhao, H., Lucas, J., Wall, T.: Characteristics of chars from low-temperature pyrolysis of lignite. Energy Fuels. **28**(1), 275–284 (2014). https://doi.org/10.1021/ef401423s
45. Akcay, C., Yalcin, M.: Morphological and chemical analysis of Hylotrupes bajulus (old house borer) larvae-damaged wood and its FTIR characterization. Cellulose. **28**(3), 1295–1310 (2021). https://doi.org/10.1007/s10570-020-03633-5
46. Bal Altuntaş, D., Nevruzoğlu, V., Dokumacı, M., Cam, Ş.: Synthesis and characterization of activated carbon produced from waste human hair mass using chemical activation. Carbon Lett. **30**, 307–313 (2020). https://doi.org/10.1007/s42823-019-00099-9
47. Traoré, M., Kaal, J., Martínez Cortizas, A.: Differentiation between pine woods according to species and growing location using FTIR-ATR. Wood Sci. Technol. **52**, 487–504 (2018). https://doi.org/10.1007/s00226-017-0967-9
48. Li, C., Kumar, S.: Preparation of activated carbon from un-hydrolyzed biomass residue. Biomass Convers. Biorefin. **6**, 407–419 (2016). https://doi.org/10.1007/s13399-016-0197-7
49. Zhang, J., Zhong, Z., Shen, D., Zhao, J., Zhang, H., Yang, M., Li, W.: Preparation of bamboo-based activated carbon and its application in direct carbon fuel cells. Energy Fuels. **25**(5), 2187–2193 (2011). https://doi.org/10.1021/ef200161c
50. Surekha, G., Krishnaiah, K.V., Ravi, N., Suvarna, R.P.: FTIR, Raman and XRD analysis of graphene oxide films prepared by modified Hummers method. In Journal of Physics: Conference Series (Vol. 1495, No. 1, p. 012012). IOP Publishing (2020)., March https://doi.org/10.1088/1742-6596/1495/1/012012
51. Lin, Q., Huang, Y., Yu, W.: An in-depth study of molecular and supramolecular structures of bamboo cellulose upon heat treatment. Carbohydr. Polym. **241**, 116412 (2020). https://doi.org/10.1016/j.carbpol.2020.116412
52. Mandal, M., Nayak, A.K., Upadhyay, P., Patra, S., Subudhi, S., Mahapatra, A., Mahanandia, P.: Hydrothermal synthesis of ZnFe2O4 anchored graphene and activated carbon as a new hybrid electrode for high-performance symmetric supercapacitor applications. Diam. Relat. Mater. **139**, 110300 (2023). https://doi.org/10.1016/j.diamond.2023.110300
53. Chayande, P.K., Singh, S.P., Yenkie, M.K.N.: Characterization of activated carbon prepared from almond shells for scavenging phenolic pollutants. Chem. Sci. Trans. **2**(3), 835–840 (2013). https://doi.org/10.7598/cst2013.358
54. Lua, A.C., Yang, T.: Effect of activation temperature on the textural and chemical properties of potassium hydroxide activated carbon prepared from pistachio-nut shell. J. Colloid Interface Sci. **274**(2), 594–601 (2004). https://doi.org/10.1016/j.jcis.2003.10.001
55. Timur, S., Kantarli, I.C., Onenc, S., Yanik, J.: Characterization and application of activated carbon produced from oak cups pulp. J. Anal. Appl. Pyrol. **89**(1), 129–136 (2010). https://doi.org/10.1016/j.jaap.2010.07.002
56. Nabais, J.V., Carrott, P.J.M., Carrott, M.R., Menéndez, J.A.: Preparation and modification of activated carbon fibres by microwave heating. Carbon. **42**(7), 1315–1320 (2004). https://doi.org/10.1016/j.carbon.2004.01.033
57. Panhwar, İ., Babar, A.A., Qureshi, S., Memon, S.A., Arain, M.: Utilization of biomass (Rice straw) to produce activated charcoal through single stage pyrolysis process. J. Int. Environ. Appl. Sci. **14**(1), 1–6 (2019)
58. Joshi, S., Pokharel, B.P.: Preparation and characterization of activated carbon from lapsi (Choerospondias axillaris) seed stone by chemical activation with potassium hydroxide. J. Inst. Eng. **9**(1), 79–88 (2013). https://doi.org/10.3126/jie.v9i1.10673
59. IkhtiarBakti, A., Gareso, P.L.: Characterization of active carbon prepared from coconuts shells using FTIR, XRD and SEM techniques. J. IIm. Pendidik. Fis. Al-Biruni. **7**, 33–39 (2018). https://doi.org/10.24042/jipfalbiruni.v%vi%i.2459
60. Köseoğlu, E., Akmil-Başar, C.: Preparation, structural evaluation and adsorptive properties of activated carbon from agricultural waste biomass. Adv. Powder Technol. **26**(3), 811–818 (2015). https://doi.org/10.1016/j.apt.2015.02.006